

Anisotropic two-dimensional metallic state of Ge(001) $c(8 \times 2)$ -Au surfaces: An angle-resolved photoelectron spectroscopy

Kan Nakatsuji,^{*} Ryota Niikura, Yuki Shibata, Masamichi Yamada, Takushi Iimori, and Fumio Komori[†]
Institute for Solid State Physics, University of Tokyo, 5-1-5 Kashiwanoha, Kashiwa-shi, Chiba 277-8581, Japan
 (Received 10 March 2009; revised manuscript received 23 July 2009; published 14 August 2009)

The electronic structure of the Ge(001) $c(8 \times 2)$ -Au surface has been investigated by means of angle-resolved photoelectron spectroscopy. The atomic structure of the surface includes nanowires along the $\langle 110 \rangle$ direction separated by deep grooves, which were observed by scanning tunneling microscopy. The dispersion relation along the $\langle 110 \rangle$ direction showed the existence of a metallic surface-state band in accordance with $8 \times$ periodicity. Moreover, the Fermi-surface measurement revealed that the band has an ellipsoidal shape, indicating an anisotropic two-dimensional metallic state. This is in contrast to the previously reported one-dimensional character of the system [J. Schäfer, C. Blumenstein, S. Meyer, M. Wisniewski, and R. Claessen, *Phys. Rev. Lett.* **101**, 236802 (2008)]. A structural model including periodic arrangement of Au adsorbed (111) nanofacets was examined by comparing the electronic structure with that of the flat Ge(111) $\sqrt{3} \times \sqrt{3}$ -Au surface.

DOI: [10.1103/PhysRevB.80.081406](https://doi.org/10.1103/PhysRevB.80.081406)

PACS number(s): 73.20.At, 79.60.Jv, 68.37.Ef, 73.61.Cw

Exploring low-dimensional electronic properties of metal-adsorbed semiconductor surfaces is one of the important subjects in surface physics. In particular, the metal-adsorbed Si and Ge surfaces are known to exhibit various kinds of two-dimensional (2D) or one-dimensional (1D) structures. In some cases, metallic surface states are found inside the bulk band gap so that their surface electronic structures have been intensively studied as ideal systems to address the low-dimensional metal. Especially, 1D metallic systems attract much interest since exotic properties are expected to appear such as charge-density wave transition due to Peierls instability and Luttinger liquid phase.¹

However, even if the surface atomic structure has a 1D morphology, it does not always exhibit 1D metallic properties. For instance, Si(001)-In surface is a 2D semiconductive system despite of atomic chain structure of the metal atoms,² and Si(112)-Ga surface has conduction channels perpendicular to the Ga atom chain.³ So far, 1D metallic systems have been realized in only a few surfaces such as Si(557), (553)-Au (Ref. 4) and Si(111)-In.⁵ Novel low-dimensional properties and their origins have been intensively studied in these systems.⁶

Search for 1D metallic systems on Ge(001) substrate has been attempted by Pt and Au adsorption.⁷⁻¹¹ The formation of Pt- or Au-contained nanowires along the $\langle 110 \rangle$ direction has been observed by scanning tunneling microscopy (STM). They commonly arrange in 1.6 nm, i.e., four times periodicity of the substrate unit cell.

On the Ge(001)-Au surface, the two adjacent nanowires make a unit of the $c(8 \times 2)$ structure^{9,10} Schäfer *et al.* found one-dimensional delocalized charge cloud on a narrow bright line of the nanowire with a single Au atom width in the topographic image of STM and a metallic surface state in angle-resolved photoelectron spectroscopy (ARPES) measurements.¹⁰ They conclude that the system has a 1D metallic state localized at a single Au atom chain on the surface. In contrast to this claim, Houselt *et al.*¹¹ reported that the nanowire has an energy gap at the Fermi energy (E_F) on the basis of their tunneling spectroscopy. In their STM observations, a deep groove was found between the bright

lines of the nanowire and is not less than 0.6 nm deep.¹¹ They proposed a structural model, “nanofacet model,” including periodic arrangement of Ge(111) $\sqrt{3} \times \sqrt{3}$ -Au (Ref. 12) nanofacets in $4 \times$ periodicity in the direction perpendicular to the bright line which is interpreted as a buckled Ge dimer row with dangling bonds on the top ridge of the nanofacets. Thus the structure and the electronic states reported so far are still controversial.

In the present study, we measured the Fermi surface of the Ge(001)-Au surface by ARPES and have found the reported metallic state anisotropic two dimensional. To verify the nanofacet model, we also studied the Ge(111) $\sqrt{3} \times \sqrt{3}$ -Au surface and found 2D metallic band. However, the dispersion relation of the metallic state in the present system does not depend on the incident photon energy and indicates an anisotropic 2D state extending in the (001) plane.

Measurements by ARPES were performed in an ultrahigh-vacuum (UHV) chamber with a hemispherical analyzer as the photoelectron detector. A He discharged lamp was used as a nonpolarized He $I\alpha$ (21.22 eV) light source. Linearly polarized synchrotron light emitted from beamline 18A in the Photon Factory at KEK was also used to vary the incident photon energy ($h\nu$) between 17 and 40 eV. The surface morphology was studied using STM in another UHV system. The base pressure of these chambers was less than 2.5×10^{-8} Pa.

Substrates of *n*-type Ge(001) and Ge(111) were cleaned by repeated cycles of 1 keV Ar⁺ sputtering at 675 K and resistive heating up to 950 K for 15 min after flashing at 1050 K for 1 min. Gold was deposited from a tungsten basket onto the clean surface kept at 675 K.

In the ARPES chamber, the deposition rate of Au was monitored by a quartz microbalance and calibrated by the intensity ratio of Au $4f$ and Ge $2p$ core-level spectra of the x-ray photoelectron spectroscopy (XPS). The XPS intensity ratio on the clean Ge(001) and (111) surfaces were plotted as a function of the deposition time. On the (111) surface, number density of Au atoms on the surface at a break in the slope was defined to be equal to that of Ge atoms on the ideal (111) 1×1 surface where a clear $\sqrt{3} \times \sqrt{3}$ pattern was

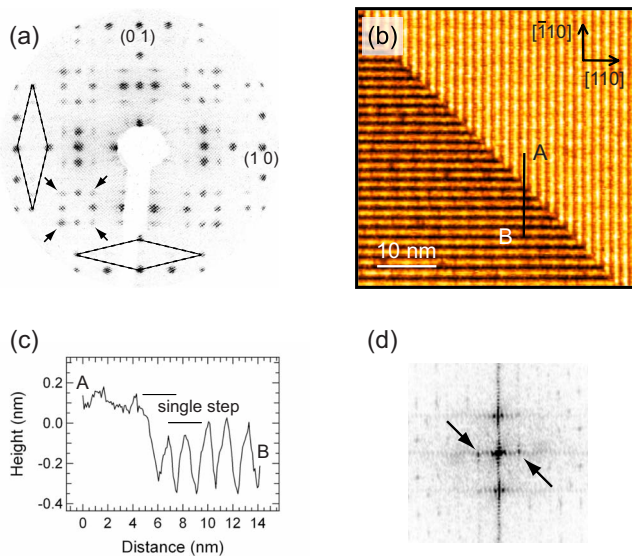


FIG. 1. (Color online) (a) A typical LEED pattern of the Ge(001) $c(8 \times 2)$ -Au surface at 130 K. Primary beam energy was 25 eV. The reciprocal unit cell of the two domains is indicated by dashed rhombuses. Small arrows show extra $8 \times$ spots, which do not trace the unit. (b) STM topographic image of the surface at RT. The size of the image is $47 \text{ nm} \times 47 \text{ nm}$. The sample bias voltage and the tunneling current were -1.2 V and 0.9 nA , respectively. (c) Cross section of the line A-B in (b). (d) FFT image of a rectangular area in the lower terrace in (b). The arrows indicate spots reflecting $8 \times$ periodicity in the nanowire direction.

observed^{12,13} in the low-energy electron diffraction (LEED). From this calibration, the Au coverage at a break in the slope on the (001) surface was estimated to be 1.1–1.2 ML. Here, a ML is defined as the same number density of atoms as that on the ideal Ge(001) 1×1 surface. A clear $c(8 \times 2)$ LEED pattern was observed below the break while above the break, additional $16 \times$ spots were found.

Figure 1(a) shows a typical double domain LEED pattern on the Ge(001) $c(8 \times 2)$ -Au surface at 130 K. In addition to the $c(8 \times 2)$ spots, extra $8 \times$ spots were observed as indicated by the arrows. These can be seen even when the coverage of Au is 0.5 ML. The pattern did not show any different periodicity between 65 and 400 K although extra $8 \times$ spots became weaker at high temperature.

The double domain of the nanowire arrangement is confirmed by an STM image at room temperature (RT) as shown in Fig. 1(b). Note that the area between the bright lines of the nanowire is imaged as a deep groove as in Fig. 1(c), which is the cross section between A and B in Fig. 1(b). The depth depended on the sample bias voltage, ranging from 0.34 to 0.46 nm. These values are smaller than reported ones,¹¹ likely because the apparent depth strongly depends on the shape of the STM tip for the highly corrugated surface such as the nanofacet model.

In some of our STM images, the arrangement of the protrusions on top of the bright lines of the nanowire corresponds to the $c(8 \times 2)$ unit cell in which the $8 \times$ periodicity is perpendicular to the nanowire as previously reported.¹⁰ However, the long-range order is absent in the present image. Indeed, a $8 \times$ spot in the direction perpendicular to the nano-

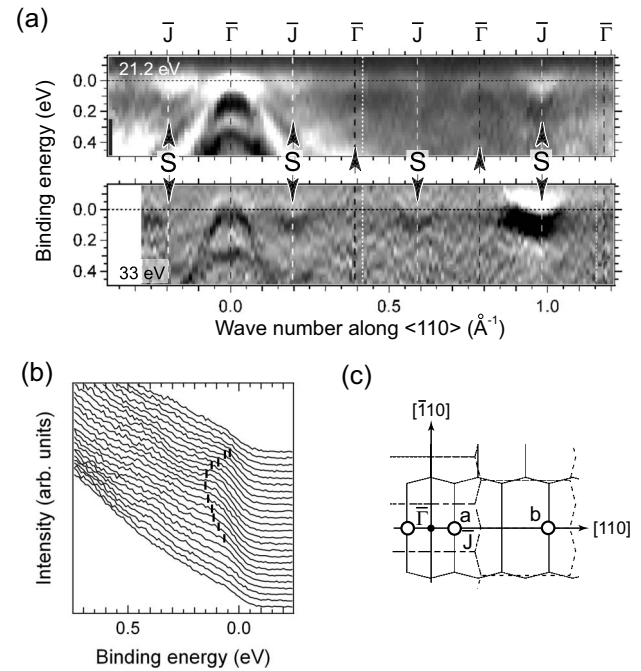


FIG. 2. (a) Valence-band structure of Au deposited Ge(001) $c(8 \times 2)$ surface at RT in the $\langle 110 \rangle$ direction. Upper and lower panels are the results at 1.3 ML of Au with $h\nu=21.22 \text{ eV}$ and at $\sim 1 \text{ ML}$ with $h\nu=33 \text{ eV}$, respectively. Photoemission intensity is larger in the darker area. Zone boundaries and $\bar{\Gamma}$ points of SBZs with $8 \times$ periodicity in this direction are indicated by white and black dashed lines, respectively. The white dotted lines are the zone boundaries of SBZs in another domain. Parabolic bands S are found at the zone boundaries (\bar{J} points) of the former domain. Faint upward double parabola indicated by arrows at $\bar{\Gamma}$ points just below E_F are due to umklapp scattering of the bulk bands (Ref. 14) by SBZs. (b) A series of ARPES spectra around $k_{||}=0.98 \text{ \AA}^{-1}$ obtained at 0.9 ML of Au with $h\nu=21.22 \text{ eV}$. The energy resolution is $\sim 60 \text{ meV}$. (c) SBZs of $c(8 \times 2)$ surface. Two domains are indicated by solid and dashed lines. The observed positions of S bands in the upper panel of (a) are also indicated by empty circles.

wire is missing in the fast-Fourier-transformed (FFT) image of the lower terrace of Fig. 1(b) as shown in Fig. 1(d). On the contrary in Fig. 1(b), we notice a $8 \times$ periodicity along the nanowire and can confirm it in the FFT image in Fig. 1(d). This means that $8 \times$ periodicities exist in the directions both perpendicular and parallel to the nanowire. Either of them is included in the observed $c(8 \times 2)$ unit cell, and the other should contribute to the extra $8 \times$ spots in the LEED pattern in Fig. 1(a).

The valence-band structure close to E_F was obtained from the second derivative of the ARPES spectra recorded in the $\langle 110 \rangle$ direction at RT as shown in Fig. 2(a). Note that the signals from both of the two domains are included. Just below E_F , parabolic surface-state bands S are clearly detected in the bulk band gap. As shown in Fig. 2(b), the band has its bottom at the binding energy (E_B) of 0.14 eV, and disperses toward and crosses E_F where the Fermi cutoff was clearly observed. No significant Au coverage dependence was observed in the S band dispersion between 0.9 and 1.3 ML. These bands locate around $k_{||}=-0.2, 0.2, 0.59$ and 0.98 \AA^{-1}

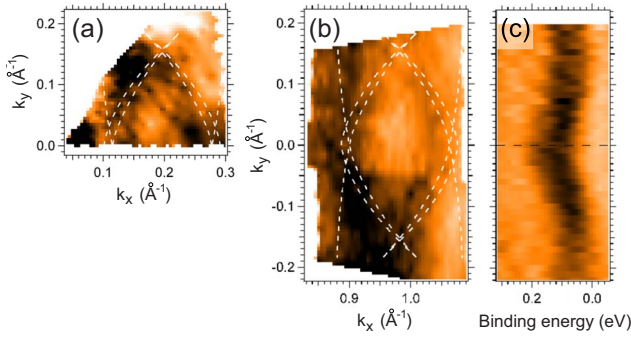


FIG. 3. (Color online) (a) and (b) Constant energy surface at $E_B=0.02$ eV obtained from the photoelectron intensity plot of the S band in a narrow energy window (0.01 eV) around two \bar{J} points, a and b in Fig. 2(c), respectively, measured at 130 K with $h\nu=21.22$ eV to improve the energy resolution. The Au coverage is 1.1 ML. Horizontal axis corresponds to $\langle 110 \rangle$ direction. The photoemission intensity is larger in darker area. (c) Dispersion relation at $k_x=0.95$ \AA^{-1} obtained from the second derivative of ARPES spectra measured at RT with $h\nu=33$ eV. See the text for details.

which correspond to \bar{J} points of the surface Brillouin zone (SBZ) with the $8\times$ periodicity along $[110]$ direction [solid lines in Fig. 2(c)]. This means that the surface is metallic in the $8\times$ periodic direction. In Ref. 10, only the band at $k_{\parallel}=0.2$ \AA^{-1} was reported.

To clarify the dimensionality of the S band, we measured the constant energy surface of the band at 0.02 eV below E_F around \bar{J} points, a and b in Fig. 2(c), as shown in Figs. 3(a) and 3(b), respectively. In the figures, the horizontal axis is the wave number in the $\langle 110 \rangle$ direction and the vertical is that perpendicular to it. The dispersion in the k_y direction at $k_x=0.95$ \AA^{-1} is shown in Fig. 3(c).

As clearly seen in Fig. 3(c), the band has parabolic dispersion not only along k_x axis but also along k_y axis. Note that another band with little dispersion appears just below E_F at larger wave numbers than ~ 0.15 \AA^{-1} in Fig. 3(c). Moreover as in Figs. 3(a) and 3(b), the Fermi surface has an oval shape; the metallic band crosses E_F at $k_x \sim \pm 0.07$ \AA^{-1} and $k_y \sim \pm 0.14$ \AA^{-1} from \bar{J} point of the SBZ. Thus, anisotropic two dimensionality of the surface electronic structure is concluded.

One of the possible origins for the 2D metallic surface band is in the nanofacet model. This model includes the $\text{Ge}(111)\sqrt{3}\times\sqrt{3}$ -Au surface, which has a Au trimer per unit cell^{12,13} and is expected to have a 2D electronic structure since $\text{Si}(111)$ -Au or -Ag and $\text{Ge}(111)$ -Ag surfaces with the $\sqrt{3}\times\sqrt{3}$ reconstruction commonly have 2D metallic band around $\bar{\Gamma}$ point.¹⁵⁻¹⁷ Hence, we have performed ARPES measurement of the $\text{Ge}(111)\sqrt{3}\times\sqrt{3}$ -Au surface as a reference.

Figure 4(a) shows the constant energy surface just below E_F at $E_B=0.02$ eV measured at RT around $\bar{\Gamma}$ point of the second SBZ locates at $(k_x, k_y)=(1.05, 0)$ (\AA^{-1}) [see Fig. 4(c)]. The dispersion relation at $k_y=0$ \AA^{-1} is shown in Fig. 4(b).

In Fig. 4(a), the Fermi surface exhibits doubled hexagons slightly distorted to a round shape with their edge perpendicular to $\bar{\Gamma}-\bar{M}$ line. The Fermi wave numbers (k_F 's) of outer

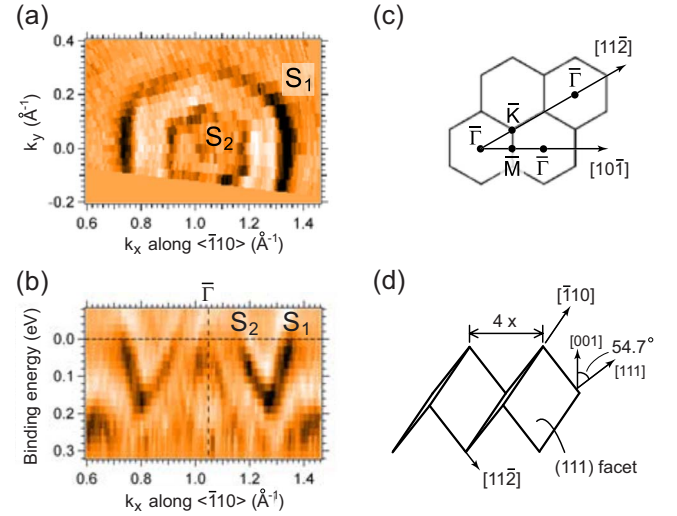


FIG. 4. (Color online) (a) and (b) Electronic structure of the $\text{Ge}(111)\sqrt{3}\times\sqrt{3}$ -Au surface close to E_F measured at RT with $h\nu=21.22$ eV. The darker area corresponds to the larger photoemission intensity. (a) Constant energy surface obtained from the second derivative of the ARPES spectra around $\bar{\Gamma}$ point of the second SBZ at $E_B=0.02$ eV. The horizontal axis corresponds to the $\bar{\Gamma}-\bar{M}$ line. Outer and inner bands are labeled as S_1 and S_2 , respectively. (b) Dispersion relation along $\bar{\Gamma}-\bar{M}$. (c) SBZs of the $\sqrt{3}\times\sqrt{3}$ surface. (d) Schematic illustration of the nanofacet model. The ridge and groove structure elongates in the $[\bar{1}10]$ direction with the $4\times$ periodicity. The $[11\bar{2}]$ direction on the (111) nanofacet is projected to the $[110]$ direction on the (001) plane. The angle between the nanofacet and the (001) plane is 54.7° .

(S_1) and inner (S_2) Fermi surfaces are ~ 0.3 \AA^{-1} and ~ 0.14 \AA^{-1} , respectively. In Fig. 4(b), the outer band S_1 has its bottom of the parabola at $\bar{\Gamma}$ point with $E_B \sim 1.0$ eV (not shown here). The inner band S_2 can have its top of the parabola also at $\bar{\Gamma}$ point as if it had a hole pocket. The hybridization of these bands is not clearly observed. Almost the same dispersion relations of S_1 and S_2 were observed along $\bar{\Gamma}-\bar{K}(\langle 11\bar{2} \rangle)$ line. These observations clearly show 2D character of the band structure of the $\text{Ge}(111)\sqrt{3}\times\sqrt{3}$ -Au surface.

Now, we will compare the observed anisotropic 2D bands in the $\text{Ge}(001)$ -Au system with those of the $\text{Ge}(111)$ -Au surface based on the nanofacet model.¹¹ Here we define ridge and groove lines with (111) nanofacets formed along the $\langle 110 \rangle$ direction as schematically shown in Fig. 4(d).

If the 2D band S_1 in the (111) nanofacet is observed in the experiment, its projected Fermi surface on the (001) plane can appear as an anisotropic 2D band. Moreover, the expected k_F 's on the (001) plane should largely depend on the incident photon energies.¹⁸ In the case of $h\nu=21.22$ eV, the Fermi surfaces expected by considering the scattering of $8\times$ periodicity in the final state show good correspondence with the experimental results as shown by white dashed curves in Figs. 3(a) and 3(b). However, this is not the case for other several $h\nu$'s between 17 and 40 eV because there is no significant change in the k_F 's as shown in Figs. 2 and 3 for $h\nu=33$ eV. Therefore, the wave function of the S band ex-

tends in the (001) plane and has anisotropic 2D character even if the atomic structure exhibits that of the nanofacet model.

The observed effective mass (m^*) of the S band is larger in k_y direction than in k_x direction. The band appears in accordance with $8\times$ periodicity, which are found both in the perpendicular and parallel directions to the nanowire as discussed using Fig. 1. In the nanofacet model, the larger m^* in the k_y direction can originate from the ridge and groove structure, which may limit the motion of the electrons.

In summary, we have investigated the electronic structure of the Ge(001) $c(8\times 2)$ -Au surface by means of ARPES. The STM image shows the arrangement of nanowires in the $\langle 110 \rangle$ direction separated by deep grooves. We found $8\times$ periodicity in the directions both perpendicular and parallel to the nanowire. The dispersion relation along the $\langle 110 \rangle$ direction shows the existence of metallic surface state in accordance with the $8\times$ periodicity. Moreover, the Fermi-

surface measurement revealed the ellipsoidal shape of the band. These observations indicate the presence of the anisotropic 2D metallic state at the surface. The 2D electronic structure on the Ge(111) $\sqrt{3}\times\sqrt{3}$ -Au surface, where metallic bands are found in the same energy range below E_F as in the Ge(001) $c(8\times 2)$ -Au surface, is discussed as a possible origin of the observed surface state in the nanofacet model. However, little dependence of the metallic band dispersion on the incident photon energy indicates that the band extends in the (001) plane.

The authors acknowledge Kota Tomatsu and Ayumi Harasawa for their help in the experiments and fruitful discussion. The STM images were analyzed by “EasySPM” software coded by K. Tomatsu. The present work was partly supported by grants in aid from Futaba Electronics Memorial Foundation and from JSPS [Scientific Research (A) No. 21244048].

*nakatsuji@issp.u-tokyo.ac.jp

†komori@issp.u-tokyo.ac.jp

¹F. J. Himpsel, K. N. Altmann, R. Bennewitz, J. N. Crain, A. Kirakosian, J.-L. Lin, and J. L. McChesney, *J. Phys.: Condens. Matter* **13**, 11097 (2001).

²H. W. Yeom, T. Abukawa, Y. Takakuwa, Y. Mori, T. Shimatani, A. Kakizaki, and S. Kono, *Phys. Rev. B* **53**, 1948 (1996).

³K. Yoo, S. J. Tang, P. T. Sprunger, I. Benito, J. Ortega, F. Flores, P. C. Snijders, M. C. Demeter, and H. H. Weiering, *Surf. Sci.* **514**, 100 (2002).

⁴J. N. Crain, A. Kirakosian, K. N. Altmann, C. Bromberger, S. C. Erwin, J. L. McChesney, J.-L. Lin, and F. J. Himpsel, *Phys. Rev. Lett.* **90**, 176805 (2003).

⁵H. W. Yeom, S. Takeda, E. Rotenberg, I. Matsuda, K. Horikoshi, J. Schaefer, C. M. Lee, S. D. Kevan, T. Ohta, T. Nagao, and S. Hasegawa, *Phys. Rev. Lett.* **82**, 4898 (1999).

⁶For example, J. R. Ahn, J. H. Byun, H. Koh, E. Rotenberg, S. D. Kevan, and H. W. Yeom, *Phys. Rev. Lett.* **93**, 106401 (2004); I. Barke, F. Zheng, T. K. Rügheimer, and F. J. Himpsel, *ibid.* **97**, 226405 (2006).

⁷A. A. Stekolnikov, F. Bechstedt, M. Wisniewski, J. Schäfer, and R. Claessen, *Phys. Rev. Lett.* **100**, 196101 (2008).

⁸A. van Houselt, T. Gnielka, J. M. J. Aan de Brugh, N. Oncel, D. Kockmann, R. Heid, K. Bohnen, B. Poelsema, and H. J. W.

Zandvliet, *Surf. Sci.* **602**, 1731 (2008).

⁹J. Wang, M. Li, and E. I. Altman, *Phys. Rev. B* **70**, 233312 (2004); *Surf. Sci.* **596**, 126 (2005).

¹⁰J. Schäfer, C. Blumenstein, S. Meyer, M. Wisniewski, and R. Claessen, *Phys. Rev. Lett.* **101**, 236802 (2008).

¹¹A. van Houselt, M. Fischer, B. Poelsema, and H. J. W. Zandvliet, *Phys. Rev. B* **78**, 233410 (2008).

¹²P. B. Howes, C. Norris, M. S. Finney, E. Vlieg, and R. G. van Silfhout, *Phys. Rev. B* **48**, 1632 (1993).

¹³M. Göthelid, M. Hammar, M. Björkqvist, U. O. Karlsson, S. A. Flodström, C. Wigren, and G. LeLay, *Phys. Rev. B* **50**, 4470 (1994).

¹⁴K. Nakatsuji, Y. Takagi, F. Komori, H. Kusunohara, and A. Ishii, *Phys. Rev. B* **72**, 241308(R) (2005).

¹⁵K. N. Altmann, J. N. Crain, A. Kirakosian, J.-L. Lin, D. Y. Petrovykh, F. J. Himpsel, and R. Losio, *Phys. Rev. B* **64**, 035406 (2001).

¹⁶T. Hirahara, I. Matsuda, M. Ueno, and S. Hasegawa, *Surf. Sci.* **563**, 191 (2004).

¹⁷H. M. Zhang, T. Balasubramanian, and R. I. G. Uhrberg, *Phys. Rev. B* **63**, 195402 (2001).

¹⁸J. E. Ortega, M. Ruiz-Osés, J. Cordón, A. Mugarza, J. Kuntze, and F. Schiller, *New J. Phys.* **7**, 101 (2005).